

## HYPERVELOCITY STARS. II. THE BOUND POPULATION

WARREN R. BROWN, MARGARET J. GELLER, SCOTT J. KENYON, AND MICHAEL J. KURTZ

Smithsonian Astrophysical Observatory, Cambridge, MA 02138; wbrown@cfa.harvard.edu, mgeller@cfa.harvard.edu, skenyon@cfa.harvard.edu, mkurtz@cfa.harvard.edu

AND

BENJAMIN C. BROMLEY

Department of Physics, University of Utah, Salt Lake City, UT 84112; bromley@physics.utah.edu

Received 2006 October 19; accepted 2007 January 21

### ABSTRACT

Hypervelocity stars (HVSs) are stars ejected completely out of the Milky Way by three-body interactions with the massive black hole in the Galactic center. We describe 643 new spectroscopic observations from our targeted survey for HVSs. We find a significant ( $3.5\sigma$ ) excess of B-type stars with large velocities  $+275 \text{ km s}^{-1} < v_{\text{rf}} < 450 \text{ km s}^{-1}$  and distances  $d > 10 \text{ kpc}$  that are most plausibly explained as a new class of HVSs: stars ejected from the Galactic center on bound orbits. If a Galactic center ejection origin is correct, the distribution of HVSs on the sky should be anisotropic for a survey complete to a fixed limiting apparent magnitude. The unbound HVSs in our survey have a marginally anisotropic distribution on the sky, consistent with the Galactic center ejection picture.

*Subject headings:* Galaxy: center — Galaxy: halo — Galaxy: kinematics and dynamics — Galaxy: stellar content — stars: early-type

*Online material:* machine-readable table

### 1. INTRODUCTION

HVSs are a natural consequence of a massive black hole (MBH) in a dense stellar environment like that in the Galactic center. Hills (1988) first pointed out that a stellar binary encountering the Milky Way’s central MBH can eject one member of the binary as a HVS traveling at  $\sim 1000 \text{ km s}^{-1}$ . HVSs differ from classical “runaway” stars because (1) HVSs are unbound and (2) the classical supernova ejection (Blaauw 1961) and dynamical ejection (Poveda et al. 1967) mechanisms that explain runaway stars cannot produce ejection velocities larger than  $200\text{--}300 \text{ km s}^{-1}$  for B-type stars (Leonard 1991, 1993; Portegies Zwart 2000; Davies et al. 2002; Gualandris et al. 2004; Dray et al. 2005). The first HVS discovered, by comparison, has a heliocentric radial velocity of  $+853 \text{ km s}^{-1}$  and a Galactic rest-frame velocity of at least  $+709 \pm 12 \text{ km s}^{-1}$  (Brown et al. 2005a), many times that needed to escape the Milky Way. Photometric follow-up shows that the object is a slowly pulsating B main-sequence star (Fuentes et al. 2006). Only interaction with a MBH can plausibly accelerate this  $3 M_{\odot}$  main-sequence B star to such an extreme velocity and distance ( $\sim 110 \text{ kpc}$ ).

HVSs are fascinating because they can be used to understand the nature and environs of MBHs (see the recent theoretical work of Gualandris et al. 2005; Holley-Bockelmann et al. 2005; Levin 2006; Ginsburg & Loeb 2006, 2007; Perets et al. 2007; Baumgardt et al. 2006; Sesana et al. 2006; Bromley et al. 2006; Merritt 2006; Demarque & Virani 2007; O’Leary & Loeb 2006; Gualandris & Portegies Zwart 2007; Kollmeier & Gould 2007). The trajectories of HVSs also provide unique probes of the shape and orientation of the Galaxy’s dark matter halo (Gnedin et al. 2005). Discoveries of additional HVSs (Edelmann et al. 2005; Hirsch et al. 2005; Brown et al. 2006a, 2006b) are starting to provide suggestive limits on the stellar mass function of HVSs, the origin of massive stars in the Galactic center, and the history of stellar interactions with the MBH. Clearly, a larger sample of HVSs will be a rich source for further progress on these issues.

We have designed a successful targeted survey for new HVSs. We use the 6.5 m MMT and the Whipple 1.5 m Tillinghast tele-

scopes to obtain radial velocities of faint B-type stars, stars with lifetimes consistent with travel times from the Galactic center but which should not otherwise exist in the distant halo. Four earlier HVS discoveries from this survey are published elsewhere (Brown et al. 2006a, 2006b). Here we present spectroscopic observations of 643 new HVS candidates.

Our paper is organized as follows. In § 2 we discuss our target selection and spectroscopic identifications. In § 3 we present evidence for stars ejected from the Galactic center on bound orbits. In § 4 we show that the unbound HVSs have a marginally anisotropic distribution on the sky. We conclude in § 5. Our new observations are listed in the Appendix.

### 2. DATA

#### 2.1. Target Selection

Brown et al. (2006b) describe our target selection for candidate HVSs. Briefly, we use Sloan Digital Sky Survey (SDSS) photometry to select late B-type stars by color. Figure 1 presents the HVS survey color-color selection. We use the 6.5 m MMT telescope to observe every star with  $17 < g'_0 < 19.5$  in this color range. We have observed 136 new HVS candidates and have completed the high-declination region of the SDSS Data Release 4 (DR4; Adelman-McCarthy et al. 2006). The MMT survey is now 80% complete across SDSS DR4 and covers an area of  $\sim 5000 \text{ deg}^2$  or 12% of the entire sky.

We have also carried out a new, complementary HVS survey targeting bright stars with  $15 < g'_0 < 17$  and B-type colors in the SDSS. We use the 1.5 m Tillinghast telescope and the FAST spectrograph (Fabricant et al. 1998) to observe these bright HVS candidates. We are able to survey efficiently much bluer stars with FAST because contamination from white dwarfs is less problematic at bright magnitudes. Figure 1 shows the FAST color-color selection:  $0.1 < (u' - g')_0 < 1.5$  and  $10.67(g' - r')_0 + 3.5 < (u' - g')_0 < 10.67(g' - r')_0 + 5.07$ . This region follows the stellar sequence of B-type stars in the SDSS photometric system (Fukugita et al. 1996). Following Brown et al. (2006a) we impose

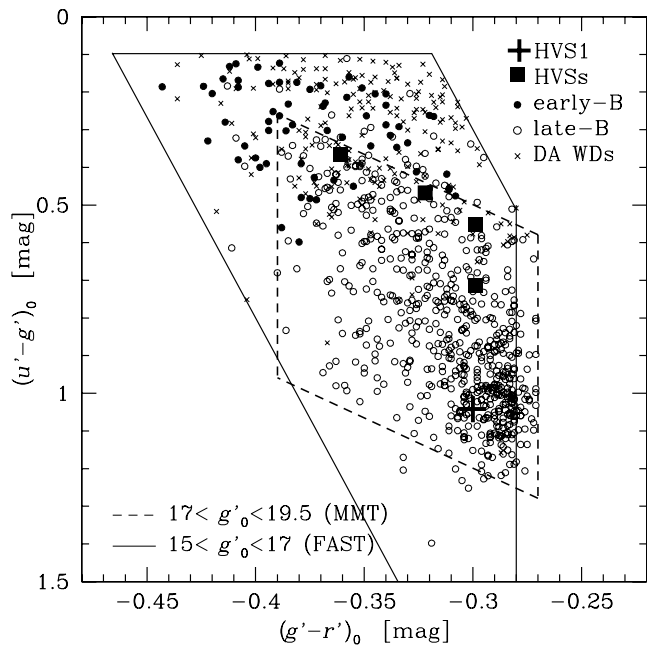


FIG. 1.—Color-color diagram showing the target selection regions for the MMT (*dashed line*) and FAST (*solid line*) samples, and the spectroscopic identifications for the combined set of 894 HVS candidates. The brighter FAST sample ( $15 < g'_0 < 17$ ) targets bluer stars and finds a number of stars with B3 and B4 spectral types (*filled circles*).

a color cut  $-0.5 < (r' - i')_0 < 0$  to reject objects with nonstellar colors. We also exclude the region of sky between  $b < -l/5 + 50^\circ$  and  $b > l/5 - 50^\circ$  to avoid excessive contamination from Galactic bulge stars. There are 746 SDSS DR4 candidate B stars  $15 < g'_0 < 17$  in the selection region. We have observed 514 stars, 69% of this total. The average surface number density of bright HVS candidates is  $0.13 \text{ deg}^{-2}$ . Thus we have surveyed an effective area of  $\sim 4000 \text{ deg}^2$  for HVS candidates  $15 < g'_0 < 17$  with FAST.

## 2.2. Spectroscopic Observations and Radial Velocities

New observations at the 6.5 m MMT telescope were obtained with the Blue Channel Spectrograph on the nights of 2006 May 23–26 and 2006 June 19–20. The spectrograph was operated with the 832 line  $\text{mm}^{-1}$  grating in second order and a  $1.25''$  slit. These settings provided wavelength coverage from 3650 to 4500 Å and a spectral resolution of 1.2 Å. Exposure times ranged from 5 to 30 minutes and were chosen to yield  $S/N = 15$  in the continuum at 4000 Å. Comparison lamp exposures were obtained after every exposure.

Observations at the 1.5 m Tillinghast telescope were obtained with the FAST spectrograph over the course of 19 nights between 2006 January 1 and 2006 July 21. The spectrograph was operated with a 600 line  $\text{mm}^{-1}$  grating and a  $2''$  slit. These settings provided wavelength coverage from 3500 to 5400 Å and a spectral resolution of 2.3 Å. Like the MMT observations, exposure times ranged from 5 to 30 minutes and were chosen to yield  $S/N = 15$  in the continuum at 4000 Å. Comparison lamp exposures were obtained after every exposure.

Spectra were extracted using IRAF<sup>1</sup> in the standard way. Radial velocities were measured using the cross-correlation package RVSAO (Kurtz & Mink 1998). Brown et al. (2003) describe

<sup>1</sup> IRAF is distributed by the National Optical Astronomy Observatory, which is operated by the Association of Universities for Research in Astronomy, Inc., under cooperative agreement with the National Science Foundation.

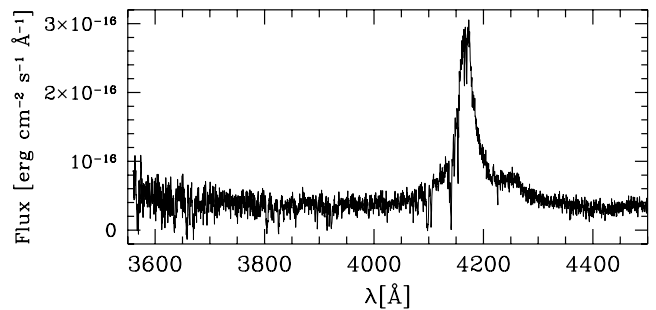


FIG. 2.—Spectrum of the  $z = 2.43$  quasar located at  $15^{\text{h}}58^{\text{m}}51.85^{\text{s}}, +22^{\circ}21'59.9''$  (J2000.0).

in detail the cross-correlation templates we use. The average uncertainty is  $\pm 11 \text{ km s}^{-1}$  for the B-type stars.

## 2.3. Selection Efficiency and Completeness

Our combined observations total 894 HVS candidates with  $15 < g'_0 < 19.5$ , of which 699 (78%) are stars of B spectral type. The remaining objects are 185 DA white dwarfs, 3 other (DZ, DB) white dwarfs, 1 compact blue galaxy (see Kewley et al. 2007), 1 quasar, and 5 objects of uncertain identification, possibly broad absorption line quasars. The one obvious quasar is a previously unobserved  $g' = 19.67$  object at  $z = 2.43$ , located at  $15^{\text{h}}58^{\text{m}}51.85^{\text{s}}, +22^{\circ}21'59.9''$  (J2000.0). Figure 2 presents its spectrum. The quasar has colors  $(u' - g')_0 = +0.80$  and  $(g' - r')_0 = -0.28$ , unusually red in  $(u' - g')_0$  and blue in  $(g' - r')_0$  compared to other quasars at similar redshifts (Schneider et al. 2005).

Figure 1 plots the spectroscopic identifications of the HVSs, other B-type stars, and the white dwarfs. Interestingly, we find stars with spectral types as early as B3 in the bright FAST sample: the filled circles in Figure 1 are the 61 stars with spectral types B3 and B4. If these early B-type stars are main-sequence stars, they are located at surprisingly large heliocentric distances,  $30 \text{ kpc} \lesssim d \lesssim 60 \text{ kpc}$ . We discuss the early B-type stars further in § 3.

Our survey is now 100% complete across the high-declination region of SDSS DR4 located at  $25^\circ < l < 210^\circ, b > 0^\circ$  in Galactic coordinates. Curiously, we find no new unbound HVSs in the completed region. Our previous discovery rate with the MMT was 1 HVS per  $\sim 50$  B-type stars (Brown et al. 2006b), yet our new set of observations contains 245 (57 from the MMT) B-type stars in the complete region. The absence of an unbound HVS in this large region suggests that the distribution of HVSs on the sky may have structure. We address the spatial distribution of HVSs in § 4.

For the remainder of this paper, we consider a “clean” sample containing 560 stars selected only from the overlapping region of color-color space:  $-0.38 < (g' - r')_0 < -0.28$  and  $2.67(g' - r')_0 + 1.30 < (u' - g')_0 < 2.67(g' - r')_0 + 2.0$ . Main-sequence B stars in this selection region will have masses of  $3\text{--}5 M_\odot$ . We also consider the full sample of 699 B-type stars at all colors. The full sample contains earlier B-type objects from the FAST sample, possibly including main-sequence stars with masses up to  $7 M_\odot$ . We emphasize that our photometric selection is complete and can detect a B-type star at any velocity.

## 3. BOUND HYPERVELOCITY STARS

The observed distribution of distances and velocities of our B-type stars provides ample evidence that they are not main-sequence runaways. Curiously, the velocity distribution reveals an asymmetry of stars with large positive radial velocities. Because the large-positive-velocity outliers are very unlikely main-sequence

runaways, we argue that the stars represent a class of *bound* HVSS ejected from the Galactic center.

### 3.1. Background

High-Galactic-latitude B-type stars were first reported by Humason & Zwicky (1947). Early spectroscopic studies (Feige 1958; Berger 1963; Greenstein 1966) showed that high-latitude B-type stars are a mix of Population II post-main-sequence stars and Population I main-sequence runaways. Accurate space motions and distances are now known for nearby  $d < 10$  kpc B-type stars observed by *Hipparcos*. A detailed analysis by Martin (2004) shows that two-thirds of the high-latitude B stars in the *Hipparcos* catalog are main-sequence runaways and one-third are evolved (mostly blue horizontal branch) halo stars. Martin (2004) finds that all of the main-sequence runaway B stars in the *Hipparcos* catalog have orbits consistent with a disk origin.

Our HVS survey probes much fainter and more distant B-type stars than observed by *Hipparcos*. Thus we cannot rely on proper motions or parallaxes. Brown et al. (2006b) discuss the nature of the late B-type stars and conclude that the distribution of radial velocities and metallicities suggests that they are likely a Galactic halo population of post-main-sequence stars and/or blue stragglers. We now revisit the possibility of main-sequence runaways in our sample.

Theorists have shown that unbinding a stellar binary through supernova disruption (Blaauw 1961) or binary-binary interactions (Poveda et al. 1967) produces a maximum ejection velocity of 200–300 km s<sup>-1</sup> (Leonard 1991, 1993; Portegies Zwart 2000; Davies et al. 2002; Gualandris et al. 2004; Dray et al. 2005). The maximum velocity is set by the escape velocity from the stellar surface. For example, a contact binary containing two  $3 M_{\odot}$  stars has a Keplerian orbital velocity of 240 km s<sup>-1</sup>. Extracting a large ejection velocity from disrupting such a system is difficult. Portegies Zwart (2000) considers supernova-unbinding binaries and finds that 90% of ejections have velocities between 0 and 100 km s<sup>-1</sup>; only 1% of  $3 M_{\odot}$  stars are ejected at 200 km s<sup>-1</sup>. Davies et al. (2002) perform similar calculations for binaries that undergo a common-envelope phase followed by a mass-transfer phase that produces a Type Ia supernova. In such systems, Davies et al. find that  $3 M_{\odot}$  secondaries have typical ejection velocities  $\sim 100$  km s<sup>-1</sup> and maximum ejection velocities of 250 km s<sup>-1</sup>. By comparison, the escape velocity of the Galaxy near the Sun is at least 500 km s<sup>-1</sup> (Carney et al. 1988; Smith et al. 2006).

Because main-sequence runaways travel on bound orbits, they spend most of their time near the apex of their trajectories above the disk with small line-of-sight velocities. For example, a star ejected at 240 km s<sup>-1</sup> vertically out of an infinite disk with surface mass density of  $95 M_{\odot} \text{ pc}^{-2}$  reaches an apex of  $z = 11$  kpc. This simple calculation illustrates that main-sequence runaways cannot simultaneously have large velocities  $v > +275$  km s<sup>-1</sup> and large distances  $z > 10$  kpc. Davies et al. (2002) use a full Galaxy potential model and compute orbits for 1000 runaway stars randomly ejected from their predicted velocity distribution. The vast majority of the Davies et al. (2002) runaways are located at  $|z| < 5$  kpc; at high Galactic latitudes  $|b| > 30^{\circ}$ , the most distant runaways are found  $\sim 25$  kpc from the disk.

### 3.2. The Asymmetric Velocity Distribution

Figure 3 plots the distribution of line-of-sight velocities, corrected to the Galactic rest frame, for our clean sample of 560 late B-type stars plus HVS1 (Brown et al. 2005a). It is apparent from Figure 3 that the velocities are well described by a Gaussian distribution. We iteratively clip  $3 \sigma$  outliers and calculate a  $105 \pm 5$  km s<sup>-1</sup> dispersion and a  $+14 \pm 4$  km s<sup>-1</sup> mean for the distri-

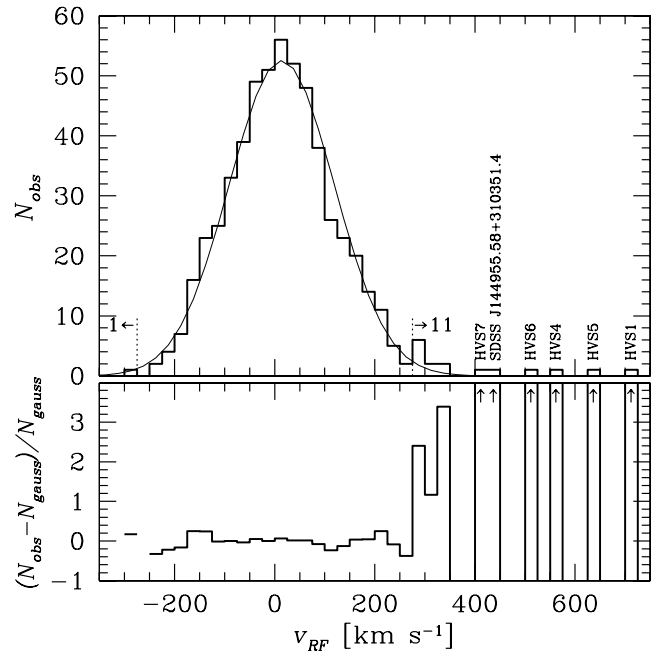


FIG. 3.— Galactic rest-frame velocity histogram of the clean sample of 560 B-type stars (top). The best-fit Gaussian (thin line) has dispersion  $105 \pm 5$  km s<sup>-1</sup>. The bottom panel plots the residuals of the observations from the best-fit Gaussian, normalized by the value of the Gaussian. In addition to the unbound HVSS, there is a significant asymmetry of 11 positive-velocity outliers with  $+275$  km s<sup>-1</sup>  $< v_{\text{rf}} < 450$  km s<sup>-1</sup>, including SDSS J144955.58+310351.4.

bution. We note that the full sample of 699 stars has a statistically identical distribution. The bottom panel of Figure 3 plots the residuals of the observations from this Gaussian distribution, normalized by the value of the Gaussian. Stars with velocities  $|v_{\text{rf}}| < 275$  km s<sup>-1</sup> show low-significance deviations from a Gaussian distribution and probably constitute a halo population of post-main-sequence stars and/or blue stragglers (Brown et al. 2006b). The highest significance outliers are the first HVS (HVS1), the four HVSSs previously discovered in this survey (HVS4–HVS7), and a new object: SDSS J144955.58+310351.4.

The possible HVS, SDSS J144955.58+310351.4, is a bright  $g'_0 = 15.70 \pm 0.03$  star with an  $A1 \pm 1.4$  spectral type and solar metallicity,  $[\text{Fe}/\text{H}]_{\text{W}_k} = -0.3 \pm 0.6$ . A main-sequence star of this type has heliocentric distance  $d \simeq 17$  kpc (Schaller et al. 1992); an evolved blue horizontal branch (BHB) star has  $d \simeq 7$  kpc (Clewley et al. 2005). Located at  $(l, b) = (48.7^{\circ}, 63.9^{\circ})$ , the star is high above the Galactic plane at  $z \simeq 15$  kpc and has a Galactocentric distance of  $R \simeq 17$  kpc (assuming  $d = 17$  kpc). The star's  $+363 \pm 10$  km s<sup>-1</sup> heliocentric radial velocity corresponds to a minimum velocity in the Galactic rest frame of  $+447$  km s<sup>-1</sup> (see Brown et al. 2006b). The star is listed with no proper motion in the USNO-B1 (Monet et al. 2003) catalog, and thus is probably bound to the Milky Way.

Curiously, we find a set of more distant stars with equally large, but bound, velocities. Figure 3 shows a significant asymmetry in the wings of the observed velocity distribution: 11 stars (excluding the 5 unbound HVSSs) have large positive velocities  $+275$  km s<sup>-1</sup>  $< v_{\text{rf}} < +450$  km s<sup>-1</sup>; only 1 star has a comparable negative velocity at  $v_{\text{rf}} = -286 \pm 12$  km s<sup>-1</sup>. This asymmetry was first pointed out by Brown et al. (2006b) but is more significant in this larger sample. There is a 0.00022 probability of drawing 11 stars with  $+275$  km s<sup>-1</sup>  $< v_{\text{rf}} < 450$  km s<sup>-1</sup> and 1 star with  $-450$  km s<sup>-1</sup>  $< v_{\text{rf}} < -275$  km s<sup>-1</sup> from a Gaussian distributions with the observed parameters. Integrating the wings of a Gaussian with the

TABLE 1  
POSSIBLE BOUND HVSSs

Catalog	$l$ (deg)	$b$ (deg)	$v_{\text{rf}}$ (km s $^{-1}$ )	Type	$R^a$ (kpc)	$R^b$ (kpc)
SDSS J074950.24+243841.2.....	196.1	23.2	+293	B8	66	27
SDSS J075055.24+472822.9.....	171.5	29.4	+307	B6	42	17
SDSS J075712.93+512938.0.....	167.0	30.9	+329	B7	32	13
SDSS J081828.07+570922.1.....	160.4	34.2	+283	B9	42	24
SDSS J090710.08+365957.5.....	186.3	42.2	+280	B9	57	29
SDSS J110224.37+025002.8.....	251.2	54.4	+326	A1	51	23
SDSS J115245.91-021116.2.....	274.9	57.5	+305	A1	53	18
SDSS J140432.38+352258.4.....	65.3	72.4	+293	B8	51	18
SDSS J141723.34+101245.7.....	357.2	63.6	+289	A1	48	19
SDSS J142001.94+124404.8.....	2.5	64.8	+300	B9	27	12
SDSS J144955.58+310351.4.....	48.7	63.9	+447	A1	16	9

<sup>a</sup> Galactocentric distance for a main-sequence star of the observed spectral type.

<sup>b</sup> Galactocentric distance for a BHB star of the observed color.

observed parameters, we would expect to find 3.6 stars with  $+275 \text{ km s}^{-1} < v_{\text{rf}} < 450 \text{ km s}^{-1}$  and 1.6 stars with  $-450 \text{ km s}^{-1} < v_{\text{rf}} < -275 \text{ km s}^{-1}$ . Thus there is an excess of  $\sim 7$  stars with large positive velocity and no apparent excess of stars with large negative velocity, significant at the  $\sim 3.5 \sigma$  level.

If the positive-velocity outliers are main-sequence stars, they are located at large distances 20–80 kpc (see Table 1). Yet the outliers cannot be runaway stars, because the runaway mechanisms cannot produce simultaneously large velocities and large distances. If, on the other hand, the positive-velocity outliers are halo stars on radial orbits, we would expect to find equal numbers of stars moving toward and away from us, contrary to observation. Compact binary systems may also produce outliers in the velocity distribution. But velocity outliers resulting from compact binaries should be distributed symmetrically, again contrary to observation. We note that neutron stars are observed traveling at velocities of  $1000 \text{ km s}^{-1}$ , but such neutron stars are the remnants of asymmetric supernova explosions, and are not B-type stars.

### 3.3. Bound HVSSs

One explanation for the significant excess of B-type stars traveling  $+275 \text{ km s}^{-1} < v_{\text{rf}} < 450 \text{ km s}^{-1}$  is the HVS mechanism. HVSSs are ejected by three-body interactions involving a MBH (Hills 1988). HVSSs almost certainly come from the Galactic center. The presence of a  $3.6 \times 10^6 M_{\odot}$  MBH (Ghez et al. 2005; Eisenhauer et al. 2005) in the crowded Galactic center inevitably produces a fountain of HVS ejections. The actual HVS ejection rate depends on the number of stars with radial orbits in the MBH’s so-called loss cone. If the MBH’s loss cone is replenished with stars scattered in by massive star clusters, molecular clouds, or intermediate-mass black holes (IMBHs; Perets et al. 2007), then the ejection rate can be orders of magnitude larger than the original Yu & Tremaine (2003) prediction. Regardless of the exact rate, this fountain picture results in a broad spectrum of HVS ejection velocities which include bound and unbound orbits (Hills 1991; Yu & Tremaine 2003; Gualandris et al. 2005; Levin 2006; Baumgardt et al. 2006; Perets et al. 2007; Sesana et al. 2006; Bromley et al. 2006; O’Leary & Loeb 2006). Bromley et al. (2006) recently calculated ejection velocities for binaries containing 3–4  $M_{\odot}$  primaries matched to our survey of B-type stars.

Over the volume sampled by our survey, Bromley et al. (2006) predict comparable numbers of HVSSs ejected into bound and unbound orbits. Our survey has discovered 4 HVSSs on unbound orbits, suggesting that  $4 \pm 2$  of our excess  $\sim 7$  positive-velocity

outliers are plausibly HVSSs on bound orbits. Although the predicted and observed numbers of bound HVSSs are statistically consistent, we note that additional HVS mechanisms may be at work. For example, O’Leary & Loeb (2006) show that single stars can be ejected by encounters with stellar-mass black holes orbiting the central MBH. Such HVSSs tend to have lower ejection velocities than HVSSs ejected by the Hills (1988) mechanism, and thus may account for additional HVSSs on bound orbits.

Figure 4 plots the Bromley et al. (2006) predicted velocity distributions for main-sequence HVSSs ejected by the central MBH as a function of Galactocentric radius. HVS velocities increase with depth because only the most rapidly moving HVSSs survive to reach large Galactocentric distances. The large squares in Figure 4 are our 4 HVSSs (*filled squares*) and the 11 stars with  $+275 \text{ km s}^{-1} < v_{\text{rf}} < 450 \text{ km s}^{-1}$  (*open squares*). We assume that the stars are main-sequence stars, and use the observed colors and spectral types of the stars to estimate stellar luminosity, distance, and stellar mass (see Table 1). The solid lines in Figure 4 indicate our survey limits for main-sequence stars of a given stellar mass.

We evaluate the probability of drawing our observed sample from the Bromley et al. (2006) predicted distributions. We use the two-dimensional, two-sample Kolmogorov-Smirnov test (Press et al. 1992) to compare the observed and predicted distributions of HVS velocity and distance. First, we generate  $10^5$  realizations of the observations—4 HVSSs plus 7 bound HVSSs randomly drawn from the 11 high-velocity outliers—and calculate the maximum difference in integrated probability against the Bromley et al. (2006) distributions. We use only the portion of the Bromley et al. (2006) distributions that fall within our observational survey limits (see Fig. 4). Second, we randomly sample 11 objects from the Bromley et al. (2006) distributions  $10^5$  times and calculate the maximum difference in integrated probabilities against the Bromley et al. (2006) distributions. Again, we use only the portion of the Bromley et al. (2006) distributions that fall within our observational survey limits. Finally, the likelihood is the fraction of time that the probabilities of the synthetic data sets exceed the probabilities of the real data sets. The mean likelihood of drawing our observed sets of stars from the predicted distributions is approximately 0.128, which neither strongly supports nor strongly rejects the Bromley et al. (2006) model. We conclude that the most plausible explanation for the observed excess of positive-velocity outliers is the HVS mechanism ejecting stars from the Galactic center on bound orbits.

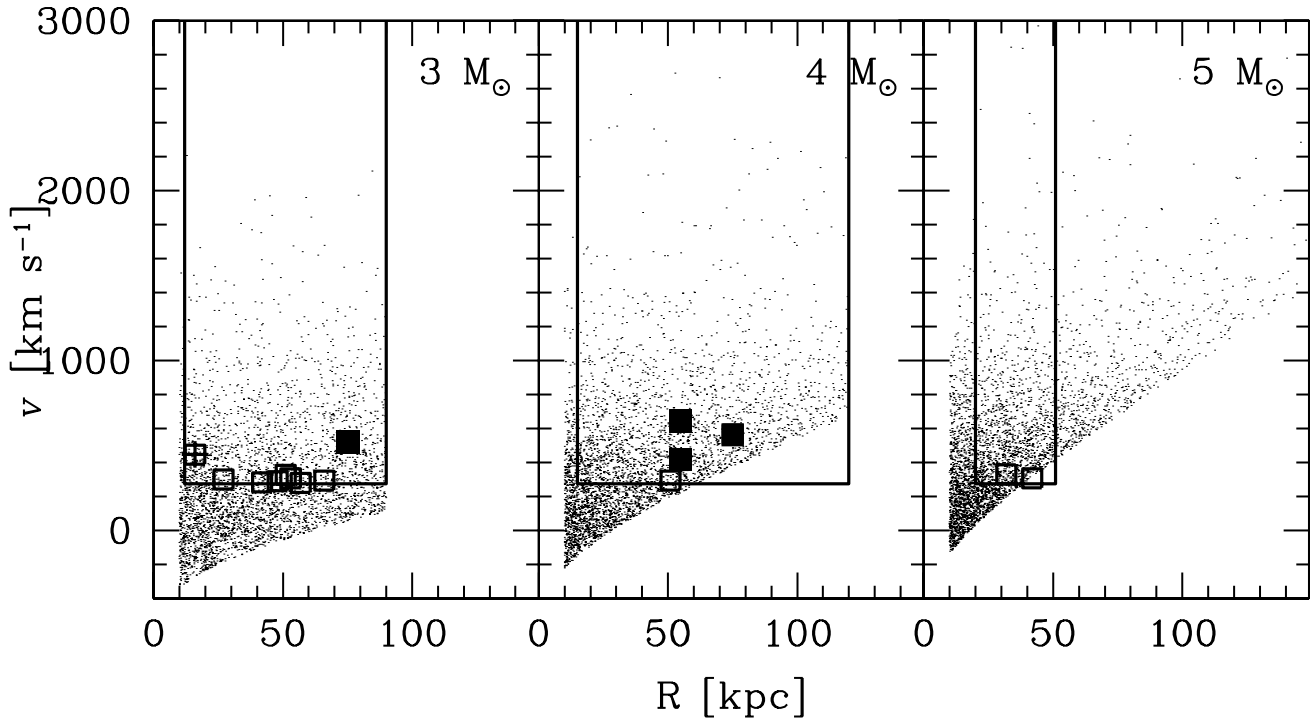


FIG. 4.—Predicted velocity distributions of  $3\text{--}5 M_{\odot}$  HVSs with distance from the Galactic center (Bromley et al. 2006). We calculate distances for our B-type stars assuming they are main-sequence stars: the four HVSs discovered by this survey (*filled squares*) and the 11 positive-velocity outliers with  $+275 \text{ km s}^{-1} < v_{\text{rf}} < 450 \text{ km s}^{-1}$  (*open squares*), including SDSS J144955.58+310351.4 (*open square with plus sign*).

We note that other stars in the literature may also be explained as bound HVSs. For example, the  $5 M_{\odot}$  main-sequence B star HIP 60350 has a heliocentric velocity of  $+230 \text{ km s}^{-1}$  and a full space velocity of  $417 \text{ km s}^{-1}$  based on *Hipparcos* measurements (Maitzen et al. 1998). The star’s large radial motion  $U = -352 \text{ km s}^{-1}$  means that it originated from well inside the solar circle, perhaps from the Galactic center.

### 3.4. Mystery of the Early B-Type Stars

Our full sample of B-type stars contains many early-type stars at bright magnitudes. Four of the early B stars in the full sample are possibly bound HVSs with  $+275 \text{ km s}^{-1} < v_{\text{rf}} < 400 \text{ km s}^{-1}$ . If they are main-sequence stars, the four early B stars have masses of  $5\text{--}7 M_{\odot}$  and they are located at distances ranging  $30\text{--}60 \text{ kpc}$  (bounded by the FAST survey limiting magnitudes). We now ask whether the number of early and late B-type bound HVSs are consistent with a standard initial mass function. Assuming the stars are main-sequence stars, there are nine  $3\text{--}5 M_{\odot}$  stars in our sample located in the same volume as the four  $5\text{--}7 M_{\odot}$  stars: a ratio of 2.25. A Salpeter initial mass function predicts a ratio of 2.7, similar to what we observe. However, the lifetimes of  $5\text{--}7 M_{\odot}$  main-sequence stars are only  $40\text{--}90 \text{ Myr}$  (Schaller et al. 1992), a factor of  $2\text{--}3$  shorter than  $3\text{--}5 M_{\odot}$  stars. The travel times of the four early B stars, assuming  $v_{\text{rf}}$  is their full space velocity, range from  $\sim 100$  to  $\sim 150 \text{ Myr}$  from the Galactic center. Thus if the early B stars are main-sequence stars ejected from the Galactic center, they do not have high enough velocities to survive to their inferred distances.

How can we reconcile the lifetimes of the early B-type stars with their travel times from the Galactic center? It is possible that the early B-type stars are blue stragglers, main-sequence stars that have undergone mass transfer or mergers. Blue stragglers are usually associated with globular clusters, yet surveys of field BHB stars in the halo find that half of the stars are in fact high-

surface-gravity blue stragglers or A dwarfs (Norris & Hawkins 1991; Preston et al. 1994; Wilhelm et al. 1999; Brown et al. 2003, 2005b; Clewley et al. 2004). Because HVSs likely originate in tight binary systems, it is possible that some HVSs experience mass transfer from their former companion prior to being ejected from the Galactic center. A blue straggler origin is one explanation for HVS2, an  $8 M_{\odot}$  HVS with a main-sequence lifetime otherwise inconsistent with travel time from the Galactic center (Edelmann et al. 2005).

It is also possible that the early B-type stars are main-sequence stars ejected elsewhere in the Galaxy by dynamical interactions with compact objects such as IMBHs. However, as the mass of a black hole decreases, the cross section of an HVS interaction decreases (e.g., Hills 1988). A stellar binary must come much closer to an IMBH before the gravitational tidal energy exceeds the binding energy of the binary. Thus an IMBH produces fewer HVSs than a MBH in the same environment. Unless IMBHs are ubiquitous in dense stellar environments such as the centers of globular clusters, we expect that the overall HVS rate is dominated by the MBH in the Galactic center.

A final possibility is that the early B-type stars are post-main-sequence stars. Demarque & Virani (2007) argue that the Galactic center contains many more old dwarf stars than young B stars, and thus the MBH should eject many more BHB stars than main-sequence B stars. Davies & King (2005) and Dray et al. (2006) argue that the Galactic center contains tidally stripped evolved stars (in effect, BHB stars with small hydrogen envelopes) that mimic B stars. B-type BHB stars with hot effective temperatures and small hydrogen envelopes spend most of their helium-burning lifetimes at intrinsically faint luminosities (Yi et al. 1997; Dray et al. 2006). Thus, if they are BHB stars, the early B-type stars are located  $10\text{--}20 \text{ kpc}$  from the Galactic center and have travel times ranging from  $25$  to  $50 \text{ Myr}$ . The BHB progenitor lifetimes easily exceed the inferred travel times, reconciling any difficulties with the MBH

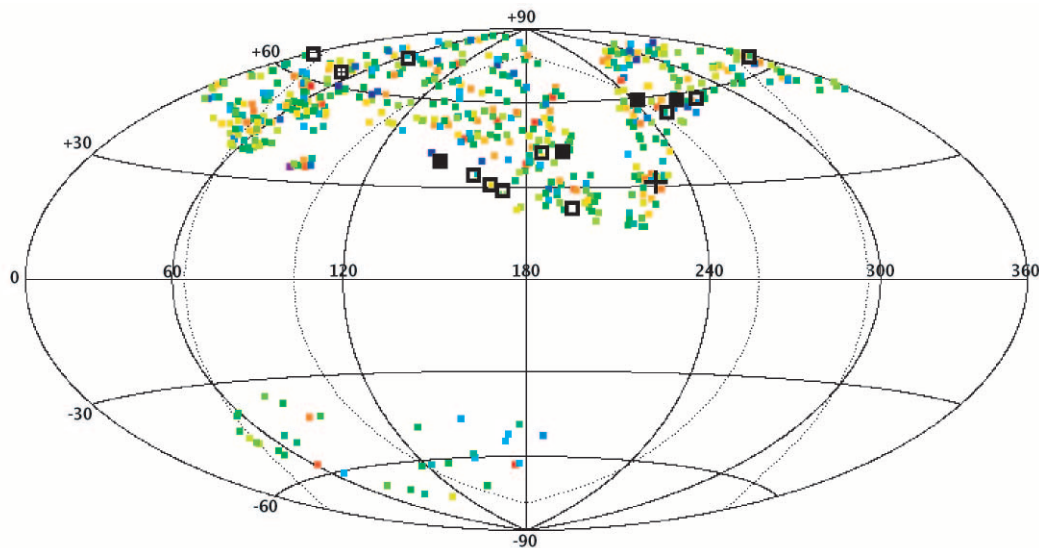


FIG. 5.— Aitoff sky map, in Galactic coordinates, showing the clean sample of 560 B-type HVS candidates. Radial velocities, in the Galactic rest frame, are indicated by the color of the filled squares: purple is  $-300$ , green is  $0$ , and red is  $+300$   $\text{km s}^{-1}$ . The HVSs are completely off this color scale and are marked by: HVS1 (*plus sign*), the four HVSs discovered by this survey (*filled squares*), and the 11 positive-velocity outliers with  $+275 \text{ km s}^{-1} < v_{\text{rf}} < 400 \text{ km s}^{-1}$  (*open squares*), including SDSS J144955.58+310351.4 (*open square with plus sign*). The dotted lines are lines of constant unbound HVS fraction calculated from the Bromley et al. (2006) models.

ejection origin. To test the post-main-sequence explanation requires high-dispersion spectroscopy to determine the stellar nature of the HVSs.

#### 4. HVS SPATIAL ANISOTROPY

The distribution of HVSs on the sky is linked to their origin. Bromley et al. (2006) show that the fraction of unbound HVSs increases with radial distance from the Galactic center (see Fig. 4). The fraction changes with depth because only the most rapidly moving HVSs survive to reach large Galactocentric distances. Because the Sun is located 8 kpc from the Galactic center, our survey reaches approximately 16 kpc deeper toward the anticenter than toward the Galactic center. Thus, if the fountain model of HVSs ejected from the Galactic center is correct, we expect to find more unbound HVSs toward the anticenter.

We use the Bromley et al. (2006) models (Fig. 4) to calculate the expected fraction of unbound HVSs in our survey volume as a function of position on the sky. The predicted fraction of unbound HVSs ranges from 53% toward the Galactic center to 63% toward the anticenter. The fraction does not vary much because it is dominated by the survey volume at large distances. The HVSs found in this survey, however, are not located at distances beyond  $\sim 80$  kpc. If we limit the survey volume to the observed range of HVS distances, then the predicted fraction of unbound HVSs ranges from 31% to 46%. We now consider the observations.

Figure 5 plots the distribution of our clean sample of 560 B-type stars across the sky in Galactic coordinates. Color indicates the radial velocity, in the Galactic rest frame, of the stars. The four unbound HVSs (*filled black squares*) discovered by this survey are completely off the color scale; HVS1 is marked by a plus sign. The 11 possible bound HVSs are indicated by open squares; SDSS J144955.58+310351.4 is plotted with an open square with a plus sign. The dotted lines in Figure 5 are lines of constant HVS fraction calculated from the Bromley et al. (2006) models. We note that our survey is currently incomplete in the SDSS equatorial slices, located at  $l > 210^\circ$  and  $b < 0^\circ$ .

It is striking that all of the unbound HVSs in our survey are located toward the anticenter. We randomize the observed velocities among the positions of all 560 stars, and find a 0.064 probability of

randomly drawing the 4 unbound HVSs from our survey in the hemisphere  $90^\circ < l < 270^\circ$ . Thus the unbound HVSs have a marginally anisotropic spatial distribution, being preferentially located in the anticenter hemisphere with  $\sim 2\sigma$  confidence. We note that the 3 unbound HVSs not from this survey, HVS1 (Brown et al. 2005a), HVS2 (Edelmann et al. 2005), and HVS3 (Hirsch et al. 2005), are also located in the anticenter hemisphere  $90^\circ < l < 270^\circ$ .

The 11 possible bound HVSs, on the other hand, appear more evenly distributed across the sky: 6 bound HVSs are located at  $90^\circ < l < 270^\circ$  and 5 bound HVSs are located at  $|l| < 90^\circ$ . To calculate the variation in unbound HVS fraction, we consider only 7 bound HVSs (the excess number of high velocity outliers in Fig. 3) and split them 4/3 between the anticenter and Galactic-center hemispheres, respectively. The fraction of unbound HVSs is then  $50\% \pm 30\%$  in the anticenter hemisphere and  $0\% \pm 40\%$  in the Galactic-center hemisphere. Although small-number statistics overwhelm our measurement, the unbound HVS fraction appears consistent with the predictions of Bromley et al. (2006) and the Galactic-center ejection picture.

There is another possible explanation for spatial anisotropy: HVSs ejected via single-star encounters with a MBH binary are preferentially ejected in the orbital plane of the MBH binary (Gualandris et al. 2005; Holley-Bockelmann et al. 2005; Levin 2006; Sesana et al. 2006; Merritt 2006; Baumgardt et al. 2006). Recent  $N$ -body simulations for the case of an IMBH inspiraling into a MBH, however, show that HVSs are ejected nearly isotropically because the angular momentum vector of the IMBH rapidly changes on a  $\sim 1$  Myr timescale (Baumgardt et al. 2006). Moreover, our observed set of HVSs do not share common travel times from the Galactic center. Different IMBH inspiral events would likely have different orbital histories; thus it seems unlikely that the observed HVS spatial distribution can point back to a binary MBH origin. A set of HVSs with common travel times must be found in order to test the binary MBH origin.

#### 5. CONCLUSIONS

We discuss our targeted survey for HVSs, a spectroscopic survey of stars with B-type colors. We introduce a new component of the survey that samples brighter and bluer stars using

the FAST spectrograph. Our combined set of observations now contains 699 stars of B spectral type, 188 white dwarfs, and 1 previously unidentified  $z = 2.43$  quasar located at  $15^{\text{h}}58^{\text{m}}51.85^{\text{s}}$ ,  $+22^{\circ}21'59.9''$  (J2000.0).

We find no new unbound HVSs, but we find evidence for a new class of *bound* HVSs. The velocity distribution of the B-type stars shows a significant asymmetry: an excess of  $\sim 7$  stars with large positive velocities  $+275 \text{ km s}^{-1} < v_{\text{rf}} < 450 \text{ km s}^{-1}$  and no apparent excess of stars with large negative velocity, significant at the  $\sim 3.5 \sigma$  level. Neither halo stars on radial orbits, compact binary stars, nor main-sequence runaway stars ejected from the disk can explain simultaneously the large velocities and distances of these stars. The most plausible explanation is that the positive velocity outliers are HVSs ejected from the Galactic center on bound orbits.

Our bright FAST survey contains a large number of early B-type stars, four of which have velocities  $+275 \text{ km s}^{-1} < v_{\text{rf}} < 450 \text{ km s}^{-1}$ . These four possible bound HVSs have main-sequence lifetimes too short to survive to their inferred distances, however. One explanation is that the stars are post-main-sequence stars. Establishing HVSs as main-sequence or post-main-sequence stars is important for measuring the stellar mass function of HVSs and probing the types of stars that orbit near the MBH. Stellar rotation is a useful discriminant between rapidly rotating main-sequence B stars (Abt et al. 2002; Martin 2004) and slowly rotating BHB stars (Peterson et al. 1995; Behr 2003). Metallicity is also a good discriminant between young main-sequence B stars and post-main-sequence halo stars. Echelle observations of the brightest HVSs, underway now, will reveal the stars' true nature.

A Galactic-center origin predicts that unbound HVSs should be found preferentially toward the anticenter as a result of survey selection. We observe that the unbound HVSs have a marginally anisotropic distribution at  $2 \sigma$  confidence. Our estimates of un-

bound HVS fraction are consistent with the Galactic-center ejection picture. Measuring the spatial distribution of a larger sample of HVSs may provide a strong test of the stars' origin.

We note that full space motions for the HVSs will be known in a few years. A *Hubble Space Telescope* program is measuring the stars' positions with 0.5 mas accuracies by registering background galaxies across Advanced Camera for Surveys images. The HVSs have predicted proper motions of  $0.5\text{--}1 \text{ mas yr}^{-1}$ ; thus  $3 \sigma$  proper-motion measurements are possible over a 3 year baseline (Gnedin et al. 2005).

We are continuing our targeted HVS survey of faint B-type stars. SDSS Data Release 5 provides additional targets that we are now following up with the MMT and Whipple 1.5 m telescopes. Given our current discovery rate, we expect to find another few unbound HVSs in the coming months. Identifying HVSs throughout the Galaxy will allow us to measure the mass function of stars in the Galactic center and the history of stellar interactions with the central MBH.

We thank M. Alegria, J. McAfee, and A. Milone for their assistance with observations obtained at the MMT Observatory, a joint facility of the Smithsonian Institution and the University of Arizona. We thank H. Perets and S. Sigurdsson for helpful correspondence. This project makes use of data products from the Sloan Digital Sky Survey, which is managed by the Astrophysical Research Consortium for the Participating Institutions. This research has made use of NASA's Astrophysics Data System Bibliographic Services. This work was supported by W. Brown's Clay Fellowship and the Smithsonian Institution.

*Facilities:* MMT (Blue Channel Spectrograph), FLWO:1.5m (FAST Spectrograph)

## APPENDIX

### DATA TABLE

Table 2 lists the 643 new observations from our HVS survey, excluding the extragalactic objects; 134 HVS candidates were observed with the MMT and 509 were observed with FAST (see § 2). Table 2 includes columns of right ascension and declination coordinates (J2000.0),  $g'$  apparent magnitude,  $(u' - g')_0$  and  $(g' - r')_0$  color, and our heliocentric velocity  $v_{\text{helio}}$ . The column WD indicates whether the object is a B-type star (WD = 0) or a white dwarf (WD = 1).

We note that  $(u' - g')_0$  color correlates strongly with the observed spectral type of the B-type stars. Our spectral types are completely independent of the SDSS photometry. We classify spectral types based on O'Connell (1973) and Worthey et al. (1994) line indices as described in Brown et al. (2003). Typical uncertainty is  $\pm 1.6$  spectral subtypes. Figure 6 plots our spectral types and the  $(u' - g')_0$  color for our full sample of 699 B-type stars. The solid line is the best-fit relation: spectral type =  $9.5(u' - g')_0 + 11.5$ , where spectral type 10 = B0, 15 = B5, 20 = A0, etc. The spectral types of the stars in our HVS survey range B3–A2, with a dispersion around the best-fit relation of  $\pm 1$  spectral subtypes or  $\pm 0.1$  mag in  $(u' - g')_0$ .

TABLE 2  
HVS SURVEY: NEW OBSERVATIONS

R.A. (J2000.0)	Decl. (J2000.0)	$g'$ (mag)	$(u' - g')_0$ (mag)	$(g' - r')_0$ (mag)	WD	$v_{\text{helio}}$ ( $\text{km s}^{-1}$ )
12 52 48.84	52 16 04.1	$18.030 \pm 0.028$	$0.506 \pm 0.039$	$-0.365 \pm 0.036$	0	$-102 \pm 10$
12 56 04.39	60 52 43.1	$18.410 \pm 0.029$	$0.521 \pm 0.041$	$-0.293 \pm 0.036$	1	$-61 \pm 36$
13 01 02.56	61 02 23.5	$19.527 \pm 0.029$	$0.414 \pm 0.047$	$-0.362 \pm 0.036$	1	$17 \pm 39$
13 19 47.37	51 20 14.5	$18.443 \pm 0.012$	$0.631 \pm 0.029$	$-0.328 \pm 0.021$	0	$-72 \pm 10$

NOTES.—Units of right ascension are hours, minutes, and seconds, and units of declination are degrees, arcminutes, and arcseconds. Table 2 is published in its entirety in the electronic edition of the *Astrophysical Journal*. A portion is shown here for guidance regarding its form and content.

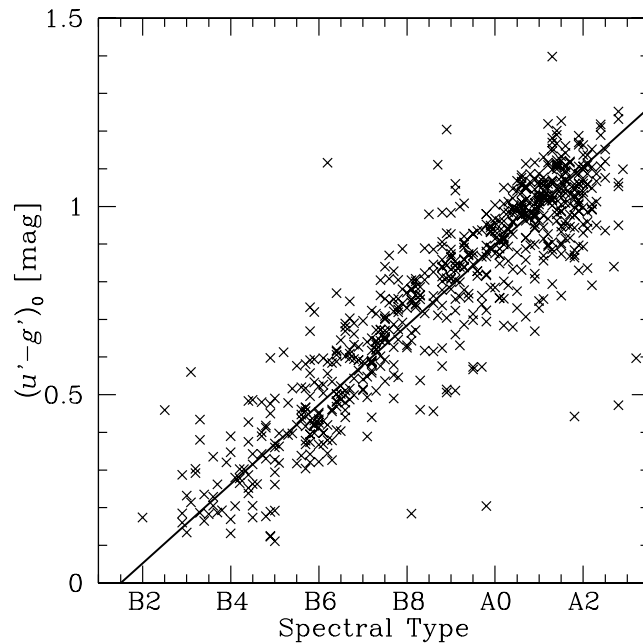


Fig. 6.—Spectral types determined from our spectroscopy and SDSS  $(u' - g')_0$  color for the full sample of 699 B-type stars.

#### REFERENCES

- Abt, H. A., Levato, H., & Grosso, M. 2002, *ApJ*, 573, 359  
 Adelman-McCarthy, J. K., et al. 2006, *ApJS*, 162, 38  
 Baumgardt, H., Gualandris, A., & Portegies Zwart, S. 2006, *MNRAS*, 372, 174  
 Behr, B. B. 2003, *ApJS*, 149, 67  
 Berger, J. 1963, *PASP*, 75, 393  
 Blaauw, A. 1961, *Bull. Astron. Inst. Netherlands*, 15, 265  
 Bromley, B. C., Kenyon, S. J., Geller, M. J., Barcikowski, E., Brown, W. R., & Kurtz, M. J. 2006, *ApJ*, 653, 1194  
 Brown, W. R., Allende Prieto, C., Beers, T. C., Wilhelm, R., Geller, M. J., Kenyon, S. J., & Kurtz, M. J. 2003, *AJ*, 126, 1362  
 Brown, W. R., Geller, M. J., Kenyon, S. J., & Kurtz, M. J. 2005a, *ApJ*, 622, L33  
 ———. 2006a, *ApJ*, 640, L35  
 ———. 2006b, *ApJ*, 647, 303  
 Brown, W. R., Geller, M. J., Kenyon, S. J., Kurtz, M. J., Allende Prieto, C., Beers, T. C., & Wilhelm, R. 2005b, *AJ*, 130, 1097  
 Carney, B. W., Laird, J. B., & Latham, D. W. 1988, *AJ*, 96, 560  
 Clewley, L., Warren, S. J., Hewett, P. C., Norris, J. E., & Evans, N. W. 2004, *MNRAS*, 352, 285  
 Clewley, L., Warren, S. J., Hewett, P. C., Norris, J. E., Wilkinson, M. I., & Evans, N. W. 2005, *MNRAS*, 362, 349  
 Davies, M. B., & King, A. 2005, *ApJ*, 624, L25  
 Davies, M. B., King, A., & Ritter, H. 2002, *MNRAS*, 333, 463  
 Demarque, P., & Virani, S. 2007, *A&A*, 461, 651  
 Dray, L. M., Dale, J. E., Beer, M. E., Napiwotzki, R., & King, A. R. 2005, *MNRAS*, 364, 59  
 Dray, L. M., King, A. R., & Davies, M. B. 2006, *MNRAS*, 372, 31  
 Edelmann, H., Napiwotzki, R., Heber, U., Christlieb, N., & Reimers, D. 2005, *ApJ*, 634, L181  
 Eisenhauer, F., et al. 2005, *ApJ*, 628, 246  
 Fabricant, D., Cheimets, P., Caldwell, N., & Geary, J. 1998, *PASP*, 110, 79  
 Feige, J. 1958, *ApJ*, 128, 267  
 Fuentes, C. I., Stanek, K. Z., Gaudi, B. S., McLeod, B. A., Bogdanov, S., Hartman, J. D., Hickox, R. C., & Holman, M. J. 2006, *ApJ*, 636, L37  
 Fukugita, M., Ichikawa, T., Gunn, J. E., Doi, M., Shimasaku, K., & Schneider, D. P. 1996, *AJ*, 111, 1748  
 Ghez, A. M., Salim, S., Hornstein, S. D., Tanner, A., Lu, J. R., Morris, M., Becklin, E. E., & Duchene, G. 2005, *ApJ*, 620, 744  
 Ginsburg, I., & Loeb, A. 2006, *MNRAS*, 368, 221  
 ———. 2007, *MNRAS*, in press (astro-ph/0609440)  
 Gnedin, O. Y., Gould, A., Miralda-Escudé, J., & Zentner, A. R. 2005, *ApJ*, 634, 344  
 Greenstein, J. L. 1966, *ApJ*, 144, 496  
 Gualandris, A., & Portegies Zwart, S. 2007, *MNRAS*, 376, L29  
 Gualandris, A., Portegies Zwart, S., & Eggleton, P. P. 2004, *MNRAS*, 350, 615  
 Gualandris, A., Portegies Zwart, S. P., & Sipior, M. S. 2005, *MNRAS*, 363, 223  
 Hills, J. G. 1988, *Nature*, 331, 687  
 ———. 1991, *AJ*, 102, 704  
 Hirsch, H. A., Heber, U., O'Toole, S. J., & Bresolin, F. 2005, *A&A*, 444, L61  
 Holley-Bockelmann, K., Sigurdsson, S., Mihos, C. J., Feldmeier, J. J., Ciardullo, R., & McBride, C. 2005, preprint (astro-ph/0512344)  
 Humason, M. L., & Zwicky, F. 1947, *Contrib. Mt. Wilson/Carnegie Obs.*, 724, 1  
 Kewley, L. J., Brown, W. R., Geller, M. J., Kenyon, S. J., & Kurtz, M. J. 2007, *AJ*, 133, 882  
 Kollmeier, J. A., & Gould, A. 2007, *ApJ*, submitted (astro-ph/0701350)  
 Kurtz, M. J., & Mink, D. J. 1998, *PASP*, 110, 934  
 Leonard, P. J. T. 1991, *AJ*, 101, 562  
 ———. 1993, in *ASP Conf. Ser. 45, Luminous High-Latitude Stars*, ed. D. D. Sasselov (San Francisco: ASP), 360  
 Levin, Y. 2006, *ApJ*, 653, 1203  
 Maitzen, H. M., Paunzen, E., Pressberger, R., Slettebak, A., & Wagner, R. M. 1998, *A&A*, 339, 782  
 Martin, J. C. 2004, *AJ*, 128, 2474  
 Merritt, D. 2006, *ApJ*, 648, 976  
 Monet, D. G., et al. 2003, *AJ*, 125, 984  
 Norris, J. E., & Hawkins, M. R. S. 1991, *ApJ*, 380, 104  
 O'Connell, W. O. R. 1973, *AJ*, 78, 1074  
 O'Leary, R. M., & Loeb, A. 2006, *MNRAS*, submitted (astro-ph/0609046)  
 Perets, H. B., Hopman, C., & Alexander, T. 2007, *ApJ*, 656, 709  
 Peterson, R. C., Rood, R. T., & Crocker, D. A. 1995, *ApJ*, 453, 214  
 Portegies Zwart, S. F. 2000, *ApJ*, 544, 437  
 Poveda, A., Ruiz, J., & Allen, C. 1967, *Bol. Obs. Tonantzintla Tacubaya*, 4, 860  
 Press, W. H., Teukolsky, S. A., Vetterling, W. T., & Flannery, B. P. 1992, *Numerical Recipes in C: The Art of Scientific Computing* (2nd ed.; Cambridge: Cambridge Univ. Press)  
 Preston, G. W., Beers, T. C., & Shectman, S. A. 1994, *AJ*, 108, 538  
 Schaller, G., Schaerer, D., Meynet, G., & Maeder, A. 1992, *A&AS*, 96, 269  
 Schneider, D. P., et al. 2005, *AJ*, 130, 367  
 Sesana, A., Haardt, F., & Madau, P. 2006, *ApJ*, 651, 392  
 Smith, M. C., et al. 2006, *MNRAS*, submitted (astro-ph/0611671)  
 Wilhelm, R., Beers, T. C., Sommer-Larsen, J., Pier, J. R., Layden, A. C., Flynn, C., Rossi, S., & Christensen, P. R. 1999, *AJ*, 117, 2329  
 Worthey, G., Faber, S. M., Gonzalez, J. J., & Burstein, D. 1994, *ApJS*, 94, 687  
 Yi, S., Demarque, P., & Kim, Y.-C. 1997, *ApJ*, 482, 677  
 Yu, Q., & Tremaine, S. 2003, *ApJ*, 599, 1129